EXPLORING MOTOR IMAGERY EEG PATTERNS FOR STROKE PATIENTS WITH DEEP NEURAL NETWORKS

Dawei Cheng[†]*, Ye Liu*[†] *and Liqing Zhang*[†]

[†]Key Laboratory of Shanghai Education Commission for Intelligent Interaction and Cognitive Engineering, Dep. of Computer Science and Engineering, Shanghai Jiao Tong University, China

ABSTRACT

Studies show that motor imagery based Brain-Computer Interface (BCI) systems can be utilized therapeutically in stroke rehabilitation. Efficient decoding of subjects' motor intentions is essential in BCI-based rehabilitation systems to manipulate a neural prosthesis or other devices for motor relearning. However, due to cortical reorganization, the desynchronization potential evoked by the motor imagery of patients with brain lesions is quite different from that evoked by the motor imagery of normal subjects. These differences can be attributed to active cortex regions, frequency bands and amplitude. In this paper, we use a deep learning method to explore the EEG patterns of key channels and the frequency band for stroke patients. The EEG data is bandpass filtered into multiple sub-bands split by a sliding window strategy. Under these sub-bands, diverse spatial-spectral features are extracted and fed into a deep neural network for classification, uncovering the spectral patterns (bandpass filters) and spatial patterns (spatial weights). Experimental results from five stroke patients show that our method has higher classification accuracy than several state-of-the-art approaches. By tracking gradual changes in EEG patterns during rehabilitation, we try to uncover the neurophysiological plasticity mechanism in the impaired cortexes of stroke patients.

***Index Terms*—** Deep Learning, Brain-Computer Interface (BCI), EEG, Stroke

1. INTRODUCTION

A Brain-Computer Interface (BCI) provides a direct pathway for communication between a human brain and an external device [1]. This means that BCI technology enables stroke patients to communicate and control devices using their brain signals [2]. In addition, BCI can help stroke patients recover motor function as an effective rehabilitation tool [3, 4]. BCI can direct brain plasticity by requiring close attention to motor tasks or requiring activation or deactivation of specific brain signals.

Among a variety of brain-diffused signals, the most commonly used in BCI is scalp and noninvasively recorded electroencephalogram (EEG). Motor imagery EEG studies are widely emerged due to their discriminative property and inexpensive acquisition. One of the novel applications in motor imagery research is to use BCI technology as a supplementary rehabilitation therapy for stroke patients [5, 6]. In order to use EEG signals to control neural prostheses or other devices for the rehabilitation of post-stroke arm motion incoordination, a reliable prediction of the subject's motion intent must be provided. Enormous signal processing and classification algorithms have been reported [7, 8, 9].

Cortical reorganization during recovery means that the motor imagery patterns of stroke patients can differ significantly from those of normal subjects [10, 11]. Such differences can be attributed to active cortex regions, frequency bands and amplitude. Some fMRI and PET studies have reported dynamic changes in the EEG pattern during recovery, which may deviate from those of healthy subjects [12, 13]. Thus, the cortical regions mainly involved in performing motor imagery may vary over time. Moreover, some studies report that active rhythms may migrate and modulate in the affected hemisphere during rehabilitation [11]. For example, a higher-frequency band may contribute largely to motor imagery in the early stages of recovery, but the importance decentralizes and partly distributes to lower bands over time. Therefore, traditional *manual* feature selection and extraction methods for EEG requiring specified domain knowledge usually fails when applied to stroke patients.

Recent developments in deep learning techniques allow *automatic* feature extraction and feature selection, and can eliminate the limitation of manual features. Deep architecture models have achieved successful results in many tasks, especially in speech and image domains, and outperform shallow models (e.g. logistic regression, multilayer perception, support vector machine) [14, 15, 16]. In recent years, deep learning methods have been successfully applied to EEG, electromyogram, ECG, skin resistance and other physiological

The work was supported by the National Basic Research Program of China (2015CB856004), the Key Basic Research Program of Shanghai Science and Technology Commission, China (15JC1400103, 16JC1402800)

signal processing fields. These methods achieve results comparable to other conventional methods [17, 18, 19].

In this paper, to explore the EEG patterns of stroke patients, we propose a deep learning framework to *automatically* select the subject-specific operational frequency band and channels group, improving the classification performance. Raw EEG is first filtered into multiple-frequency sub-bands. Under these sub-bands, diverse spatial-spectral features are constructed; these are fed into a deep neural network for classification.

In conclusion, the main contributions of this paper can be summarized as follows:

- To the best of our knowledge, this is the first study to use a deep learning framework for *strokes*' EEG classification that attempts to construct diverse spatial-spectral features under multiple-frequency sub-bands.
- To the best of our knowledge, this is the first study using a deep learning framework to explore the mysterious motor imagery EEG patterns in spatial and spectral domains in stroke patients.
- By tracking gradual changes in EEG patterns during rehabilitation, we try to uncover the neurophysiological plasticity mechanism in the impaired cortexes of stroke patients.

2. METHOD

The deep learning framework is proposed to classify EEG signals into two classes: left imaging and right imaging, simultaneously identifying the critical frequency bands and channels in stroke patients. We describe our framework in four parts: data acquisition, data preprocessing, feature extraction, and classification and channel-frequency selection with deep learning.

2.1. Data Acquisition

We collect EEG data from five patients with unilateral paralyzed stroke who diseased within two months. They perform 24 motor imagery tests of their disabled (left or right) arms in a BCI-FES rehabilitation training system for two months (three times a week). We record the EEG data by a 16-channel g.USBamp amplifier at a sampling rate of 256Hz. The 16 channels are: C1C6, CP3, CPZ, CP4, CZ, FC3, FCZ, FC4, P3, P4 and PZ. Patients are required to complete five courses of basic motor imagery related tasks. Each lesson consists of 40 trials lasting 240 seconds. At the beginning of each trial, a bold arrow (left or right) appears at random as a visual cue that contains a command instructing the patient to imagine moving the arrow left or right. Thereafter, an interval of two seconds is allowed between trials, during which the subjects can adjust their mental state and prepare for subsequent trials. We extract a time period starting from 0.5s to 4.5s after the cue for analysis.

2.2. Data Preprocessing

Before feature extraction, a preprocessing stage is required for the EEG data to improve the low signal-to-noise ratio (SNR). The EEG trial is bandpass filtered in a specific frequency band that relates primarily to that performing of motor imagery. For healthy people, the typical spectral characteristics of EEG in motor imagery tasks are α rhythm (813Hz) and β rhythm (1430Hz). This decreases during movement or in preparation for movement and increases after movement and during relaxation. These phenomena occur in the sensorimotor area (centro-parietal lobes) [20, 7]. However, it is not possible to obtain the spectral characteristics of stroke patients [11, 12, 13]. Thus, the EEG data from stroke patients is filtered in a broad band ranging from 5 to 40Hz.

2.3. Sub-bands PSD Features Extraction

We propose a sub-bands PSD (SBPSD) method to extract spatial-spectral features by computing the multiple power spectral density (PSD) [21] of each channel by varying frequency sub-bands in order to explore the unknown patterns of critical frequency bands and channels in stroke patients. We denote the channel set as $\mathcal{C}$. In order to extract diverse features, the EEG data in each channel $C \in \mathcal{C}$ is first filtered into multiple-frequency sub-bands; this is split by a sliding window strategy under a global frequency band G (like [5, 40]Hz in this paper). Representing B as a sub-band, we split the global band G and $\mathcal{D}$ into a universal set that includes all possible sub-bands generated by splitting. Note that the splitting procedure is supervised under the following three kinds of constraints:

- Cover: $\cup_{B \in \mathcal{D}} B = G$
- Length: $\forall B = [l, h] \in \mathcal{D}$, $L_{min} \leq h - l \leq L_{max}$, where L_{min} and L_{max} are two constants to determine the length of B
- Overlap: $\forall B_{min} = [l, l+1] \subset G, \exists B_1, B_2 \in \mathcal{D}, B_{min} \subseteq B_1 \cap B_2$

These constraints guarantee that the set $\mathcal{D}$, consisting of finite sub-bands, will not underrepresent the original continuous interval and that each band in $\mathcal{D}$ has an appropriate length. Accordingly, a sliding window strategy is proposed to produce $\mathcal{D}$.

$$\mathcal{B}_i = Slide(L_i, S_i, W_i, T_i) \tag{1}$$

After filtering EEG data of channel $C \in \mathcal{C}$ in sub-band $B \in \mathcal{B}$, PSD feature $\{\mathrm{PSD}_C^B\}$ is calculated and then fed into a deep neural network.

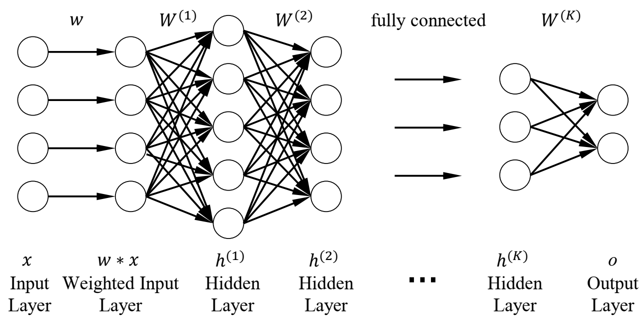

Fig. 1. Network structure of deep learning framework.

Table 1. Mean classification accuracies of the two months obtained by all the methods on five stroke patients (%)

Sub	Mon	PSD-SVM	CSP-SVM	SBCSP-SVM	CSP-DNN	SBPSD-SVM	**SBPSD-DNN**
S1	M1	47.4	52.5	58.5	57.6	58.3	**68.4**
	M2	52.3	54.6	60.2	61.2	63.6	**72.9**
S2	M1	54.6	55.7	62.6	64.6	63.3	**72.8**
	M2	58.7	56.7	65.6	68.6	69.6	**78.6**
S3	M1	42.7	53.6	57.7	60.8	61.4	**75.8**
	M2	58.7	67.2	69.8	68.6	71.4	**80.2**
S4	M1	44.6	51.9	54.6	55.5	58.7	**69.5**
	M2	48.1	54.6	58.2	61.6	65.2	**68.7**
S5	M1	58.4	59.6	65.1	66.4	67.5	**71.4**
	M2	62.7	62.4	68.3	69.1	68.7	**74.5**
Mean	M1	49.5	54.6	59.7	60.9	61.8	**71.5**
	M2	56.1	59.1	64.4	65.8	67.7	**74.9**

2.4. Classification and Channel-frequency Selection with Deep Learning

We propose a deep neural network, which is shown in Fig. 1, that enables variable feature selection in order to identify the key channel-frequency features that have non-linear behaviors. In this model, a *one-to-one* layer is added between input and the first hidden layer, where the input feature $x_j = \{\mathrm{PSD}_C^B\}_\mathrm{j}$ is connected only to the j-th node. Denoting $*$ as element-wise multiplication, then, the output of the one-to-one layer becomes $w * x$. In order to select critical frequency and channel, w, representing features scores, must be sparse.

Then, the objective function is minimized as below,

$$\min_{\theta} f(\theta) = l(\theta) + \lambda_1(\|w\|_1) + \lambda_2(\sum_{k=1}^{K+1} \|W\|_1) \tag{2}$$

where model parameter $\theta = \{w, W^{(1)}, \ldots, W^{(K+1)}\}$, K is the number of hidden layers and $W^{(k)}$ is the weight matrix connecting the $k-1$th layer to the kth layer. The log-likelihood function $l(\theta)$ in Equation 2 is

$$l(\theta) = -\sum_{j=1}^{N} \log p(y_i|h_i^{(K)}) = -\sum_{j=1}^{N} \log \frac{e^{-w_{y_i}^{(K+1)^T} h_j^{(K)}}}{\sum_{c=1}^{C} e^{-w_c^{(K+1)^T} h_j^{(K)}}} \tag{3}$$

For a given input sample x_j, $h_j^{(K)}$ is the output of K-th hidden layer. Regularization term $\lambda_1\|w\|_1$ controls the sparsity of w. Another regularization term, $\lambda_2\|W\|_1$, helps reduce the model complexity and improve optimization performance. λ_1 and λ_2 are estimated by cross validation.

It is well known in the machine learning community that Equation 2 is non-convex, while the classic back-propagation method converges only to a local minimum of the weight space. In particular, it performs quite well for a small number of hidden layers. Therefore, in this situation, we use a back-propagation algorithm to train the model. In contrast, for a large value of K, we use a stacked contractive autoencoder or deep belief network. It is preprocessed in a greedy hierarchical layer-wise algorithm and then fine-tuned by back-propagation [22].

Once the model is fine trained, we reserve the channel sets $\mathcal{C}$, frequency sub-bands $\mathcal{B}$, and the feature scores w. Then, we calculate a quantitative vector $L_\mathrm{C} = \sum_{B\in\mathcal{B}} w_C^B$ to represent the classification weight of each channel C in the set $\mathcal{C}$, where w_C^B represents the feature score of feature PSD_C^B. Similarly, the weight of each sub-frequency band is calculated and then projected onto [5, 40]. Finally, the contributed channel groups and active frequency bands with larger weights are identified.

3. EXPERIMENTAL RESULTS

In this section, we present our experimental results obtained from the five stroke patients. The feasibility and robustness of the proposed method are verified when the unknown information of the stroke patient's moving image is decoded. The experimental results are mainly reflected in two aspects: (1) the accuracy of two kinds of motor imagery EEG classification; (2) to explore the mechanism of neurophysiological plasticity.

3.1. Classification Accuracy

We denote our method as SBPSD-DNN for simplification. For comparison, five state-of-the-art algorithms are utilized for feature extraction and classification, respectively; these are: PSD combined with SVM (PSD-SVM); Common Spatial Patterns (CSP) [7] combined with SVM (CSP-SVM); the sub-band CSP (SBCSP) [23] combined with SVM (SBCSP-SVM); CSP combined with DNN (CSP-DNN), and SBPSD combined with SVM (SBPSD-SVM).

For PSD, the power spectral density value is calculated as a distinguishing feature from unidirectional EEG data (time) by fast Fourier transform. The frequency band is set from 5Hz to 40Hz. CSP is used to extract discriminant features from bi-directional EEG data (channel $\times$ time).

The number of CSP channels is set to 10. For SBCSP settings, we use 24 Gabor filters, each with a bandwidth of 4Hz, as described in the study [23]. The dimensionality of SBPSD-DNN features is 658. In SBPSD-DNN, we set K to 4 and the

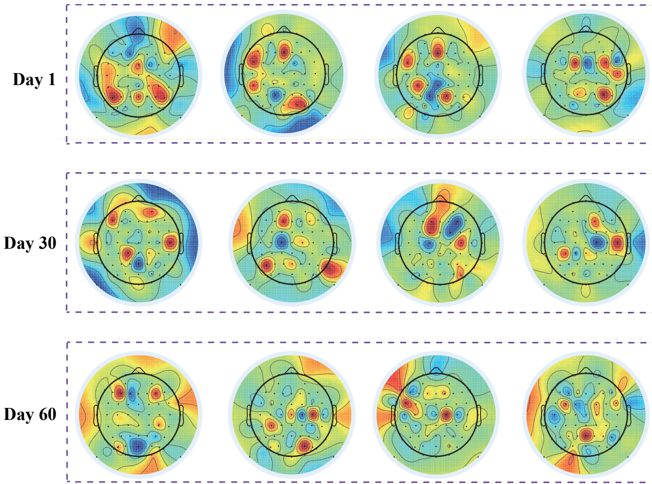

Fig. 2. CSP spatial patterns for Patient 3 on days 1, 30 and 60 (from top to bottom: day 1, 30 and 60). The red dot indicate a higher weight while blue dots represent a lower weight.

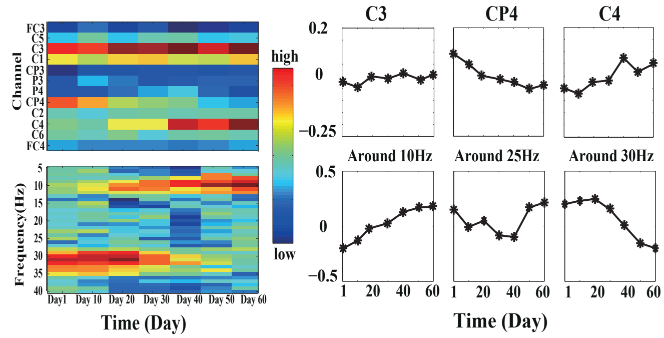

Fig. 3. The weights of the 16 channels and frequency band 5-40Hz within 7 days selected from Patient 3. All values are normalized for comparison. Left: the weight of channels and frequency bands for selected 7 days, where the red rectangle represents a larger value and the blue one represents a lower value. Right: the changes of weights minus the average of three chosen channels C3, CP4, C4 and frequencies 10Hz, 25Hz, 30Hz over the selected 7 days. Note: (1) the weight differences between channel C4 and lower frequency 10Hz gradually increase, while the weight difference of channel C3 remains unchanged; (2) the weight differences between CP4 and 30Hz higher frequency channel show a decreasing tend.

number of neurons in each hidden layer is (256,128,64,16). The cost function is described in Equation 2.4. We use 70% of data for training and the rest 30% for testing in the cross validation process.

For every patient, we calculate the mean classification accuracy in each month using different methods. Table 1 shows the mean accuracies of the two months achieved by all the methods on the five patients. We find that our proposed methods outperform all the other algorithms. With the same classification algorithm, SBPSD feature is more effective than other features. Meanwhile, DNN methods often gain higher accuracy compared to SVM.

3.2. Uncovering the Neurophysiological Plasticity Mechanism

The motor imagery EEG patterns of stroke patients change during rehabilitation. In order to observe the gradual change of EEG patterns over time, we describe spatial and spectral patterns (e.g., channel weights and frequency weights) on a two-dimensional graph. We select 7 days (days 1, 10, 20, 30, 40, 50, and 60) of the original EEG to represent different stages of the rehabilitation process. Fig. 3 shows the channel weights and frequency bands for the seven days selected by patient 3 with an impaired right cortex. For comparison purposes, Fig. 2 shows the spatial filters of days 1, 30, and 60 learned by the CSP from patient 3.

From these photographs, we can find that the spatial filters obtained by CSP look messy at first glance and, from a neurophysiological point of view, have large weights at several unexpected locations. Conversely, using the methods we proposed, we find that a larger area of the affected hemisphere was activated during rehabilitation. The importance of sensorimotor regions in affected hemispheres increases over time, while the importance of unaffected hemispheres remains unchanged. For example, in the early stages of rehabilitation, the central parietal lobe (CP4) plays a compensatory role, but its importance decreases over time. The active region gradually moves back to the central lobe (C4). Some fMRI and PET studies report similar phenomena [24]. With respect to spectral characteristics, a high-frequency band of 3035 Hz contributes greatly to motor imagery, but the importance is dispersed and partially distributed to the low-frequency band over time. This dynamic band enhancement means that the activity rhythm may be regulated during rehabilitation, as also reported in [11].

4. CONCLUSION

In this paper, a deep learning framework is proposed to explore the motor imagery EEG patterns in stroke patients. The EEG data is first bandpass filtered into a plurality of sub-bands by a sliding window strategy. In these sub-bands, different spatial-spectral features are then extracted and fed into a deep neural network to reveal spatial patterns (spatial weights) and spectral patterns (bandpass filters). Experimental results from five stroke patients show that our method has higher classification accuracy than several other state-of-the-art approaches. We uncover the neurophysiological plasticity mechanism in the impaired cortexes by tracking gradual changes in EEG patterns during the rehabilitation process of the stroke patients.

5. REFERENCES

[1] Jonathan R Wolpaw, Niels Birbaumer, William J Heetderks, Dennis J McFarland, P Hunter Peckham, Gerwin Schalk, Emanuel Donchin, Louis A Quatrano, Charles J Robinson, Theresa M Vaughan, et al., "Brain-computer interface technology: a review of the first international meeting," *IEEE transactions on rehabilitation engineering*, vol. 8, no. 2, pp. 164–173, 2000.

[2] Jonathan R Wolpaw, Niels Birbaumer, Dennis J McFarland, Gert Pfurtscheller, Theresa M Vaughan, et al., "Brain-computer interfaces for communication and control," *Clinical neurophysiology*, vol. 113, no. 6, pp. 767–791, 2002.

[3] Jie Song, Veena A Nair, Brittany M Young, Leo M Walton, Zack Nigogosyan, Alexander Remsik, Mitchell E Tyler, Dorothy Farrar-Edwards, Kristin E Caldera, Justin A Sattin, et al., "Dti measures track and predict motor function outcomes in stroke rehabilitation utilizing bci technology," *Frontiers in human neuroscience*, vol. 9, 2015.

[4] Natalie Mrachacz-Kersting, Ning Jiang, Andrew James Thomas Stevenson, Imran Khan Niazi, Vladimir Kostic, Aleksandra Pavlovic, Sasa Radovanovic, Milica Djuric-Jovicic, Federica Agosta, Kim Dremstrup, et al., "Efficient neuroplasticity induction in chronic stroke patients by an associative brain-computer interface," *Journal of neurophysiology*, vol. 115, no. 3, pp. 1410–1421, 2016.

[5] Marc E Wolf, Anne D Ebert, and Anastasios Chatzikonstantinou, "The use of routine eeg in acute ischemic stroke patients without seizures: generalized but not focal eeg pathology is associated with clinical deterioration," *International Journal of Neuroscience*, vol. 127, no. 5, pp. 421–426, 2017.

[6] Andrea Sarasola-Sanz, Nerea Irastorza-Landa, Eduardo López-Larraz, Carlos Bibián, Florian Helmhold, Doris Broetz, Niels Birbaumer, and Ander Ramos-Murguialday, "A hybrid brain-machine interface based on eeg and emg activity for the motor rehabilitation of stroke patients," in *2017 International Conference on Rehabilitation Robotics (ICORR)*. IEEE, 2017, pp. 895–900.

[7] H. Ramoser, J. Muller-Gerking, and G. Pfurtscheller, "Optimal spatial filtering of single trial EEG during imagined hand movement," *IEEE Transactions on Rehabilitation Engineering*, vol. 8, pp. 441–446, 2000.

[8] F. Lotte and C. Guan, "Regularizing common spatial patterns to improve BCI designs: unified theory and new algorithms," *IEEE Transactions on Biomedical Engineering*, vol. 58, no. 2, pp. 355–362, 2011.

[9] Yong Zhang, Bo Liu, Xiaomin Ji, and Dan Huang, "Classification of eeg signals based on autoregressive model and wavelet packet decomposition," *Neural Processing Letters*, vol. 45, no. 2, pp. 365–378, 2017.

[10] Yukihiro Hara, "Brain plasticity and rehabilitation in stroke patients," *Journal of Nippon Medical School*, vol. 82, no. 1, pp. 4–13, 2015.

[11] S. Shahid, R.K. Sinha, and G. Prasad, "Mu and beta rhythm modulations in motor imagery related post-stroke EEG: a study under BCI framework for post-stroke rehabilitation," *BMC Neuroscience*, vol. 11, pp. 1–2, 2010.

[12] Cinzia Calautti, François Leroy, Jean-Yves Guincestre, and Jean-Claude Baron, "Dynamics of Motor Network Overactivation After Striatocapsular Stroke A longitudinal PET Study Using a Fixed-Performance Paradigm," *Stroke*, vol. 32, no. 11, pp. 2534–2542, 2001.

[13] Isabelle Loubinoux, Christophe Carel, Jérémie Pariente, Sophie Dechaumont, Jean-François Albucher, Philippe Marque, Claude Manelfe, and François Chollet, "Correlation between cerebral reorganization and motor recovery after subcortical infarcts.," *Neuroimage*, vol. 20, no. 4, pp. 2166, 2003.

[14] Kaiming He, Xiangyu Zhang, Shaoqing Ren, and Jian Sun, "Deep residual learning for image recognition," in *Proceedings of the IEEE conference on computer vision and pattern recognition*, 2016, pp. 770–778.

[15] Ross Girshick, "Fast r-cnn," in *Proceedings of the IEEE international conference on computer vision*, 2015, pp. 1440–1448.

[16] Chao Zhang, Junchi Yan, Changsheng Li, Xiaoguang Rui, Liang Liu, and Rongfang Bie, "On estimating air pollution from photos using convolutional neural network," in *Proceedings of the 2016 ACM on Multimedia Conference*. ACM, 2016, pp. 297–301.

[17] LinPeng JIN and Jun DONG, "Deep learning research on clinical electrocardiogram analysis," *SCIENTIA SINICA Informationis*, vol. 45, no. 3, pp. 398, 2015.

[18] Zhe Ren, Junchi Yan, Bingbing Ni, Bin Liu, Xiaokang Yang, and Hongyuan Zha, "Unsupervised deep learning for optical flow estimation.," in *AAAI*, 2017, pp. 1495–1501.

[19] Zhong Yin, Mengyuan Zhao, Yongxiong Wang, Jingdong Yang, and Jianhua Zhang, "Recognition of emotions using multimodal physiological signals and an ensemble deep learning model," *Computer Methods and Programs in Biomedicine*, vol. 140, pp. 93–110, 2017.

[20] Gert Pfurtscheller and Christa Neuper, "Motor imagery activates primary sensorimotor area in humans," *Neuroscience letters*, vol. 239, no. 2, pp. 65–68, 1997.

[21] P. Welch, "The use of fast Fourier transform for the estimation of power spectra: a method based on time averaging over short, modified periodograms," *IEEE Transactions on Audio and Electroacoustics*, vol. 15, no. 2, pp. 70–73, 1967.

[22] Yifeng Li, Chih-Yu Chen, and Wyeth W Wasserman, "Deep feature selection: theory and application to identify enhancers and promoters," *Journal of Computational Biology*, vol. 23, no. 5, pp. 322–336, 2016.

[23] Quadrianto Novi, Cuntai Guan, Tran Huy Dat, and Ping Xue, "Sub-band common spatial pattern (SBCSP) for brain-computer interface," in *Neural Engineering, 2007. CNE'07. 3rd International IEEE/EMBS Conference on*. IEEE, 2007, pp. 204–207.

[24] A Feydy, R Carlier, A Roby-Brami, B Bussel, F Cazalis, L Pierot, Y Burnod, and MA Maier, "Longitudinal study of motor recovery after stroke recruitment and focusing of brain activation," *Stroke*, vol. 33, no. 6, pp. 1610–1617, 2002.